

Original Research

Lactate Dehydrogenase-Inhibitors Isolated from Ethyl Acetate Extract of *Selaginella doederleinii* by Using a Rapid Screening Method with Enzyme-Immobilized Magnetic Nanoparticles

Feng Zhang^{1,†}, Huiyun Li^{1,†}, Chao Liu¹, Kun Fang¹, Yongmei Jiang¹, Mingjiang Wu², Shiji Xiao¹, Lei Zhu¹, Jiaqi Yu³, Shenge Li^{3,*}, Gang Wang^{1,*}

¹School of Pharmacy, Zunyi Medical University, 563000 Zunyi, Guizhou, China

²Department of Pharmacy, Zunyi Medical and Pharmaceutical College, 563000 Zunyi, Guizhou, China

³Department of Pharmacy, The Third Affiliated Hospital of Zunyi Medical University, 563000 Zunyi, Guizhou, China

*Correspondence: leshenge@163.com (Shenge Li); wg8855350@163.com (Gang Wang)

†These authors contributed equally.

Academic Editor: Luigi De Masi

Submitted: 20 May 2022 Revised: 17 June 2022 Accepted: 13 July 2022 Published: 26 July 2022

Abstract

Background: Lactate dehydrogenase (LDH) is one of the important enzyme systems for glycolysis and gluconeogenesis. It can catalyze the reduction and oxidation reaction between propionic acid and L-lactic acid, which is usually overexpressed in cancer cells. Therefore, inhibiting the activity of LDH is a promising way for the treatment of cancer. In this study, an effective method based on ligand fishing and ultra performance liquid chromatography-mass spectrum (UPLC-MS) was established to screen and identify active ingredients from *Selaginella doederleinii* with potential inhibitory activity for LDH. **Methods:** Firstly, LDH was immobilized on the magnetic nanoparticles (MNPs), three immobilization parameters including LDH concentration, immobilization time and pH were optimized by single factor and response surface methodology for maximum (max) immobilization yield. Then, a mixed model of galloflavin and chlorogenic acid (inhibitors and non-inhibitors of LDH) was used to verify the specificity of immobilized LDH ligand fishing, and the conditions of ligand fishing were further optimized. Finally, combined with UPLC-MS, immobilized LDH was used to simultaneously screen and identify potential LDH inhibitors from the ethyl acetate extract of *Selaginella doederleinii*. **Results:** The prepared fishing material was comprehensively characterized by scanning electron microscopy (SEM), transmission electron microscope (TEM), X-ray diffraction (XRD) and fourier transform infrared spectrometer (FT-IR). The optimal immobilization conditions were obtained as LDH concentration of 0.7 mg/mL, pH value of 4.5, and immobilization time of 3.5 h. Under these conditions, the max immobilization yield was $(3.79 \pm 0.08) \times 10^3$ U/g. The specificity analysis showed that immobilized LDH could recognize and capture ligands, and the optimal ligand fishing conditions included that the incubation time was 30 min, the elution time was 20 min, and the concentration of methanol as eluent was 80%. Finally, two LDH inhibitors, amentoflavone and robustaflavone, were screened by immobilized LDH from the ethyl acetate extract of *Selaginella doederleinii*. **Conclusions:** The study provided a meaningful evidence for discovering the bioactive constituents in ethyl acetate extract of *Selaginella doederleinii* related to cancer treatment, and this ligand fishing method was feasible for screening enzyme inhibitors from similar complex mixtures.

Keywords: lactate dehydrogenase (LDH) inhibitor; functionalized magnetic nanoparticles; *Selaginella doederleinii*; biflavonoids; ligand fishing

1. Introduction

According to data released by the Global Cancer Observatory of the International Agency for Research on Cancer, a subsidiary of the World Health Organization, the number of new cancer patients worldwide in 2020 was 19.3 million, and it is expected to increase by 30.2 million in 2040 [1]. Among all cancers, female breast cancer has surpassed lung cancer as the most common one [2]. Information on the Our World in Data website shows that an estimated 9.6 million people died of various forms of cancer in 2017. With the rising morbidity and mortality, cancer is a serious threat to human health and has become a major global public health problem [3]. Therefore, it is imperative

that the search for effective cancer drugs is accelerated.

The Warburg effect is a common feature of cancer cells, which, unlike most normal cells, tends to “ferment” glucose into lactic acid even under aerobic conditions [4]. Some scholars believe that the energy generated by excessive glycolysis supports the growth of cancer cells [5], and that the production of a large amount of lactic acid causes extracellular acidification, which leads to the invasion and metastasis of cancer cells [6]. Thus, in part, it is possible to deprive cancer cells of the energy they need to survive and hinder their invasion and metastasis by inhibiting lactate dehydrogenase (LDH) during glycolysis process [7]. LDH is the rate-limiting enzyme that catalyzes the conversion of pyruvate to lactate during glycolysis and plays a crucial role



in the Warburg effect [8]. LDHA and LDHB are two isoenzymes of LDH [9]. By inhibiting the activity of LDHA, the proliferation and migration of prostate cancer cells could be inhibited and reduced [10], and this phenomenon was also observed in ovarian cancer cells [11], hepatocellular cancer cells [12], and pancreatic cancer cells [13]. Taken together, LDHA inhibitors are one of the key drugs of interest for the treatment of cancer.

At present, several screening methods for enzyme inhibitors have been established, including computer virtual screening technology [14], spectrum effect binding [15], ligand fishing technology [16], as well as others. Because ligand fishing technology has the advantages of high efficiency, good stability, and strong specificity, it has been widely used in screening inhibitors [17]. For example, lipase was immobilized on magnetic nanoparticles (MNPs), and bamboo leaves were screened for lipase inhibitors. Three were subsequently found and identified as isoorientin, orientin, and isovitexin with inhibition rates of $56.93 \pm 1.9\%$, $57.87 \pm 0.8\%$, $43.22 \pm 0.5\%$ at a concentration of $100 \mu\text{mol/L}$, respectively [18]. Alpha-amylase was immobilized on magnetic beads and screened for alpha-amylase inhibitors in ethyl acetate extracts from *Ginkgo biloba*. Four alpha-amylase inhibitors were found and analyzed using high-performance liquid chromatography (HPLC)-photodiode array detection, high-resolution mass spectrometry, and nuclear magnetic resonance spectroscopy, and they were identified as bilobetin, isoginkgetin, ginkgetin, and sciadopitysin [19]. Similarly, acetylcholinesterase (AChE) was immobilized on the surface of MNPs and screened for AChE inhibitors in an extract from *Selaginella doederleinii*. Four inhibitors were found and analyzed using ultra-high-performance liquid chromatography/mass spectrometry (UPLC/MS) and identified as amentoflavone, robustaflavone, bilobetin, and isoginkgetin, among which IC_{50} of amentoflavone was $0.73 \pm 0.009 \mu\text{mol/L}$ [20].

Selaginella doederleinii belongs to the *Selaginella* family, which is a traditional Chinese herbal medicine usually used in folk medicine as an antitumor herb [21]. Carbohydrates, alkaloids, and flavonoids are its main chemical components [22]. Pharmacological research of *Selaginella doederleinii* mainly revolves around its antitumor effects. For example, the ethyl acetate extract of *Selaginella doederleinii* was used to investigate its anti-colorectal cancer effects, and the results showed that it inhibited the proliferation of HT-29 and HCT-116 cell lines by inducing autophagic death and apoptosis through PI3K-Akt-mTOR and AMPK alpha signaling pathways [23]. HPLC was used to analyze the ethyl acetate extract of *Selaginella doederleinii*, which mainly contained eight kinds of biflavonoids, and the extract inhibited the growth of A549 lung cancer cells through the mitochondrial apoptosis pathway, decreasing Ki67 expression and microvascular density [24]. Thus, the ethyl acetate extract contained the main active antitumor

components from this plant, but the active ingredient remained unidentified.

The discovery of active natural products from widely existing medicinal resources in nature has been an important way to develop innovative drugs [25]. Therefore, in this study, LDHA was immobilized on amino-modified MNPs, the synthesis process was optimized, and the synthesized materials were characterized. Subsequently, ethyl acetate extracts from *Selaginella doederleinii* were screened for inhibitors of LDHA using the ligand fishing technique. Finally, potential LDHA inhibitors were identified by UPLC/MS.

2. Materials and Methods

2.1 Chemicals and Instruments

LDH (subunit: LDHA, 100 U/mg) and (3-aminopropyl)triethoxysilane were acquired from Aladdin Biochemical Technology Co. (Shanghai, China). Fe_3O_4 MNPs were purchased from Alcorda Chemical Reagent Co. (Chengdu, China). Coomassie brilliant blue G250, glutaraldehyde (GA), sodium pyruvate, beta-nicotinamide adenine dinucleotide, disodium salt (NADH), and HPLC grade acetonitrile and methanol were obtained from Shanghai Maclean Biochemical Technology Co. (Shanghai, China). Chlorogenic acid, galloflavin, amentoflavone, and robustaflavone were provided by Refines Biotechnology Co. (Chengdu, China).

An Agilent 1260 equipped with diode array detector was purchased from Agilent (California, USA). ACQUITY UPLC H-Class with Quaternary Solvent Manager was from Waters (Massachusetts, USA). The 759S UV-Vis spectrophotometer equipped with a unique monochromator optical path and photoelectric converter was purchased from JINGHUA Technology Instrument Co. (Shanghai, China). The vortex meter with an amplitude of 4.5 mm (circular oscillation) was purchased from JOANLAB Experimental Instruments Co. (Zhejiang, China). A Thermo Scientific™ Multiskan™ FC microplate reader with a detection wavelength range of 340–850 nm was purchased from Thermo Fisher Scientific (Massachusetts, USA).

2.2 The Ethyl Acetate Extract of *Selaginella doederleinii*

The *Selaginella doederleinii* (Guizhou, China) powder that had passed through a 60-mesh sieve was extracted twice with 75% ethanol for 2 h under reflux. The two extracts were combined and evaporated with the excess solvent until there was no alcohol smell. Finally, it was extracted three times with ethyl acetate and dried under reduced pressure and stored at 4°C [26].

2.3 Preparation of LDH-Functionalized MNPs

LDH-functionalized MNPs were prepared according to the literature with minor modifications [27]. Fifteen volumes of 50% ethanol were added to the mixture of Fe_3O_4 magnetic nanoparticles (Fe_3O_4 MNPs) and (3-

aminopropyl)triethoxysilane (1:3 mass ratio) and vigorously stirred for 24 h at 60 °C. Then, the supernatant was discarded and the product was washed five times with water and ethanol. The product, MNPs-NH₂, was dried at 40 °C for 24 h.

One mL of 5% GA was added to an Eppendorf tube containing 3 mg of MNPs-NH₂. The mixture was then sonicated for 10 min to ensure it was uniformly dispersed and then vortexed for 4 h. Next, the solid product was collected with a magnetic strip and washed 3 times with acetate buffer pH 5 at a concentration of 100 mM. Finally, 200 μ L of LDH solution was reacted with the product for a period of time and then separated with a magnetic strip and washed three times to obtain immobilized LDH.

2.4 Characterization

Scanning electron microscopy (SEM), transmission electron microscopy (TEM), X-ray diffraction (XRD), and fourier transform infrared (FTIR) spectroscopy were used to characterize Fe₃O₄ MNPs, MNPs-NH₂ and immobilize LDH. SEM was performed using a ZEISS Sigma 500 field emission scanning electron microscope equipped with a state-of-the-art backscatter detector (Oberkochen, Germany). TEM was performed using a field emission transmission electron microscope JEM-2100F with an accelerating voltage of 200 kV by Japan Electronics Co. (Tokyo, Japan). XRD was obtained using a Rigaku UltimaV X-ray polycrystalline diffractometer equipped with a graphite monochromator with high reflection efficiency (Tokyo, Japan). FTIR spectra were analyzed using a Thermo Scientific Nicolet IS5 infrared spectrometer equipped with a temperature-controlled diode laser (Massachusetts, USA).

2.5 Relative Activity and Immobilization Yield Calculation of Immobilized LDH

A unit of LDH activity was defined as the amount of enzyme that catalyzes 1 μ mol/L of NADH per minute under the specified assay conditions. The activity of LDH increases with a decrease in absorbance. According to the literature [28], the procedure was as follows: 50 μ L NADH (0.5 mM) and 50 μ L sodium pyruvate (2.5 mM) were added to an Eppendorf tube containing 3 mg of immobilized LDH, and the reaction was carried out at 37 °C for 10 min. After removing this immobilized LDH, absorbance of the supernatant was measured at 304 nm. The decrease in absorbance of NADH at 340 nm was observed during the reaction. The maximum enzymatic activity was set at 100% and the relative enzymatic activity was calculated.

$$\text{Relative activity (\%)} = \frac{A}{A_m} \times 100\% \quad (1)$$

(Where A and A_m are the decrease and max decrease in absorbance under each set of conditions, respectively.)

The Coomassie brilliant blue method was used to measure the yield of immobilized LDH [29]. One hundred μ L of the LDH solution before and after immobilization was added to 5 mL Coomassie brilliant blue solution, reacted at room temperature for 10 min, and the absorbance was then measured at 595 nm. A standard curve of LDH content was prepared (concentration was 0.1–1.5 mg/mL). The immobilized yield of LDH was then calculated.

$$\text{Immobilization yield (U/g)} = \frac{[E] \times 100}{[M]} \quad (2)$$

(Where [E] and [M] represent the difference in the amount of LDH in the supernatant before and after immobilization and the mass of MNPs, respectively.)

2.6 Parameters Optimization for LDH Immobilization

2.6.1 Single-Factor Experiment

Three parameters including LDH concentration, pH of the LDH solution, and immobilization time were investigated to obtain the optimal conditions for LDH immobilization on Fe₃O₄ MNPs. 200 μ L of LDH solution was added to 3 mg MNPs-NH₂, incubated for several hours, and then the immobilized LDH after the reaction was washed three times with buffer. Next, Eqn. 1 in Section 2.5 was used to calculate the relative activity of immobilized LDH synthesized under different conditions. The experimental conditions were as follows: (A) LDH concentrations of 0.1–1.2 mg/mL (pH 5, immobilization time 2 h); (B) LDH solution pH 3–7 (LDH concentration of 0.6 mg/mL, immobilization time 2 h); (C) Immobilization time 1–5 h (LDH concentration of 0.6 mg/mL, pH 5).

2.6.2 Response Surface Methodology (RSM)

Based on the experimental results in the above Subsection 2.6.1, a three-factor, three-level response surface analysis experiment was designed with the relative enzyme activity (Y) as the response value. The parameters were as follows: concentrations were 0.3, 0.6, and 0.9 mg/mL, pHs were 3, 4, and 5, and incubation times were 2, 3, and 4 h. Seventeen experiments were conducted based on the above design, as shown in Table 1.

Table 1. Factors and levels for Box-Behnken Design.

Factors	Coded levels		
	−1	0	1
LDH concentration (mg/mL)	0.3	0.6	0.9
immobilization pH	3	4	5
Immobilization time (h)	2	3	4

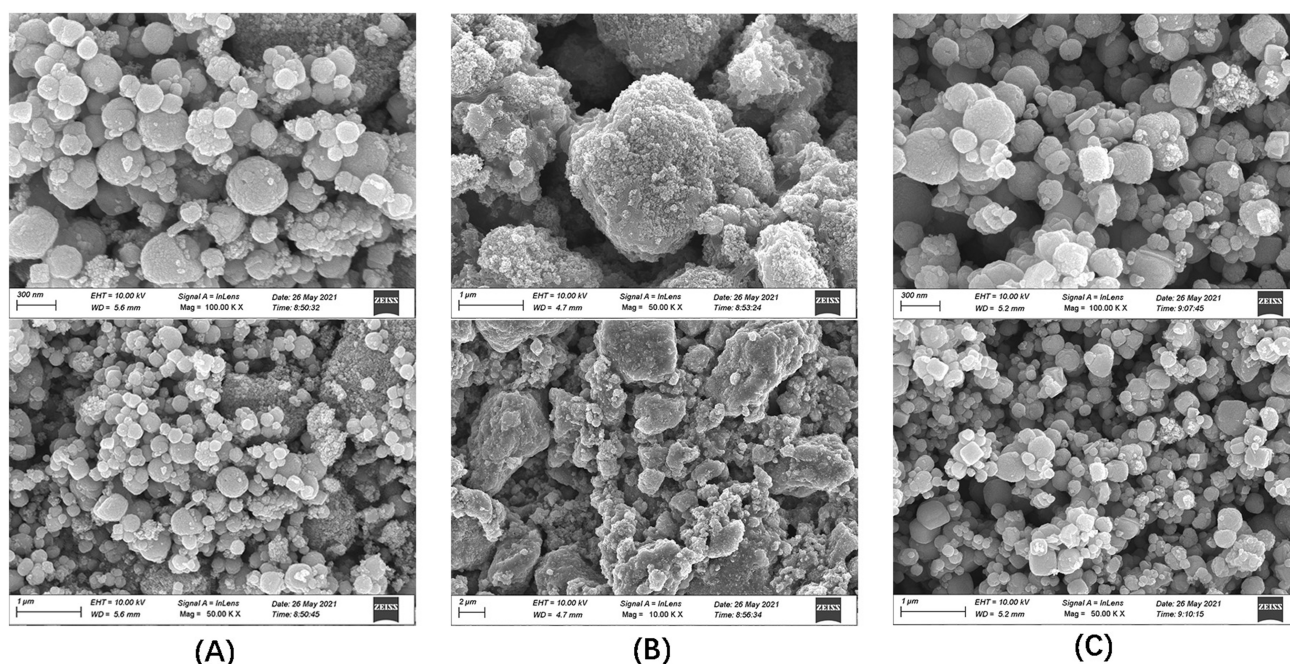


Fig. 1. SEM images of the three materials. (A) Fe_3O_4 MNPs. (B) MNPs-NH_2 . (C) Immobilized LDH.

2.7 Immobilization Yield Calculation of LDH

To clarify the relationship between the three parameters in Section 2.6.1 and the LDH immobilization yield, 100 μL of LDH supernatants before and after the reaction with 3 mg MNPs-NH_2 was used to calculate the yield using the Coomassie brilliant blue method described in Section 2.5.

2.8 Method Specificity Validation and Screening Condition

Immobilized LDH was added to a mixture containing galloflavin and chlorogenic acid (standard LDH inhibitor and non-inhibitor) for specific detection. The incubation time (10–60 min) and elution time (10–60 min) of ligand with immobilized LDH and the concentration of methanol eluent (20%–100%) were optimized. The procedure was as follows: 3 mg of immobilized LDH was added to 1 mL of a mixture of galloflavin and chlorogenic acid (S0) and incubated for 30 min. After magnetic strip separation of immobilized LDH, the supernatant was collected (S1). Next, the immobilized LDH was washed three times with 1 mL of buffer, and the washing solutions were collected (S2–S4). Then, 1 mL of methanol was added to the immobilized LDH and eluted 3 times, and the elution solution was collected each time (S5–S7). Finally, S1–S7 were analyzed using HPLC.

2.9 Screening of LDH Inhibitors from *Selaginella doederleinii* Ethyl Acetate Extracts

On the basis of the optimal ligand fishing conditions obtained in Section 2.8, 3 mg of immobilized LDH was added to 1 mL of the *Selaginella doederleinii* methanol solution (S0) and incubated for 30 min. The supernatant (S1) was then collected from the immobilized LDH. The

supernatants (S2–S4) were then collected by washing three times with 1 mL buffer. Then 1 mL methanol was used to elute three times, and the eluates were collected (S5–S7). UPLC/MS was used to analyze all samples (S0–S7).

3. Results and Discussion

3.1 Characterization

SEM is an important technique to use to observe the microscopic morphology of materials because of its great advantages in resolution, depth of field, and microstructure analysis [30]. The SEM images of Fe_3O_4 MNPs, MNPs-NH_2 , and immobilized LDH are shown in Fig. 1. Fe_3O_4 MNPs (Fig. 1A) are spherical particles with smooth surfaces and a relatively uniform distribution. After amino modification, MNPs-NH_2 (Fig. 1B) had a larger particle size, a rough surface, and a certain agglomeration. The particle size of immobilized LDH (Fig. 1C) became smaller than that of MNPs-NH_2 , but the size became more uniform and had dispersibility.

TEM uses an electron beam as a light source and an electromagnetic field as a lens to project the accelerated and concentrated electron beam onto a very thin sample. Because of the different density and thickness of the sample, images with different brightness and darkness are formed. This method is usually used for ultrastructural observation [31]. TEM images of Fe_3O_4 MNPs, MNPs-NH_2 , and immobilized LDH are shown in Fig. 2. The size distribution of Fe_3O_4 MNPs (Fig. 2A) was relatively uniform, and the agglomeration phenomenon was obvious. It could be seen in Fig. 2B that Fe_3O_4 MNPs were coated with amino groups to form MNPs-NH_2 , which increased the particle size. The particle size of immobilized LDH became smaller, but more

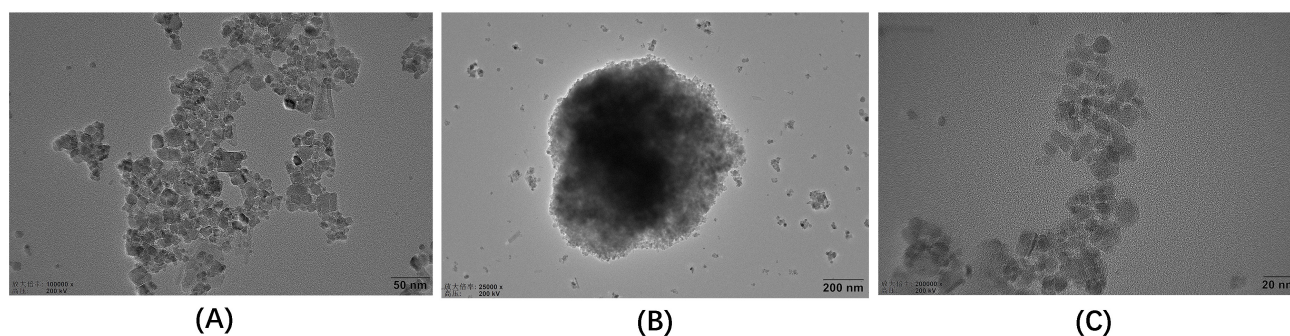


Fig. 2. TEM images of the three materials. (A) Fe_3O_4 MNPs. (B) MNPs-NH_2 . (C) Immobilized LDH.

uniform, with obvious agglomeration.

XRD is the most powerful approach applied to identify the structure of crystals and has been successfully adopted for the development of new materials [32]. The Fe_3O_4 MNPs, MNPs-NH_2 , and immobilized LDH were also characterized using XRD. As depicted in Fig. 3, the diffraction peaks at 2θ values of 30.04° , 35.08° , 43.11° , 52.89° , 56.95° , and 62.45° could be assigned as the (220), (311), (400), (422), (511), and (440) crystalline planes of Fe_3O_4 , which were consistent with the standard diffraction patterns of Fe_3O_4 species [33].

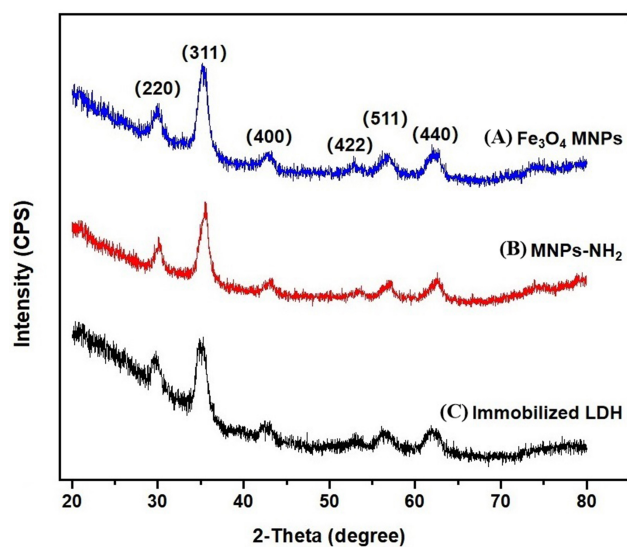


Fig. 3. XRD pattern of the three materials. (A) Fe_3O_4 MNPs. (B) MNPs-NH_2 . (C) Immobilized LDH.

FT-IR spectroscopy has the advantage of providing high resolution and decrease measurement time, so it is normally used for group structure analysis of materials and qualitative and quantitative analysis of materials [34]. This could be observed in the FT-IR images of Fe_3O_4 MNPs, MNPs-NH_2 , and immobilized LDH shown in Fig. 4. The stretching vibration of the Fe-O bond of Fe_3O_4 was observed at 576 cm^{-1} in the three materials. In the spectrum of the Fe_3O_4 MNPs, 3360 cm^{-1} and 1622 cm^{-1} cor-

responded to the stretching vibration and deformation vibration of O-H, respectively. In MNPs-NH_2 , the bending vibration peaks of Si-O, $-\text{CH}_2$, and C-H bonds were detected at 1001 cm^{-1} , 2926 cm^{-1} , and 2853 cm^{-1} , respectively. The absorption of the Si-O bond of immobilized LDH was blue-shifted and observed at 1023 cm^{-1} . Meanwhile, the absorption peaks at 1647 cm^{-1} and 1530 cm^{-1} corresponded to the stretching vibration of C=O and the bending vibration of N-H, indicating that LDH had been successfully immobilized on MNPs-NH_2 .

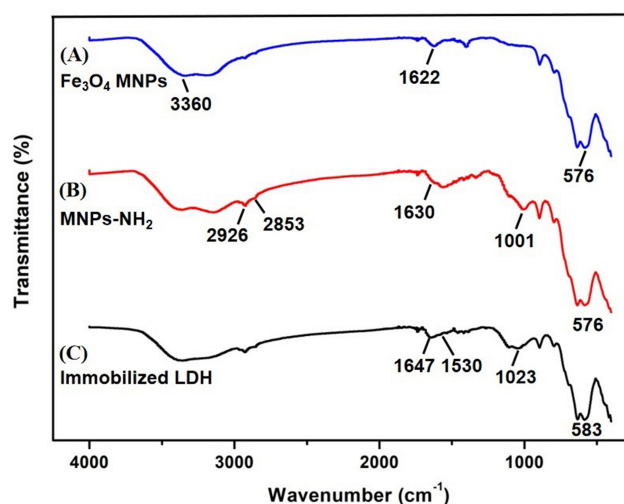


Fig. 4. FT-IR spectra of the three materials. (A) Fe_3O_4 MNPs. (B) MNPs-NH_2 . (C) Immobilized LDH.

3.2 Parameters Optimization for LDH Immobilization

LDH concentration, pH, and immobilization time in the LDH immobilization process were optimized using single-factor experiments and response surface methodology.

3.2.1 Single-Factor Experiment

The relationship between LDH concentrations, ranging from 0.1 mg/mL to 1.2 mg/mL (pH 5, immobilization time 2 h), and the relative activity of immobilized LDH

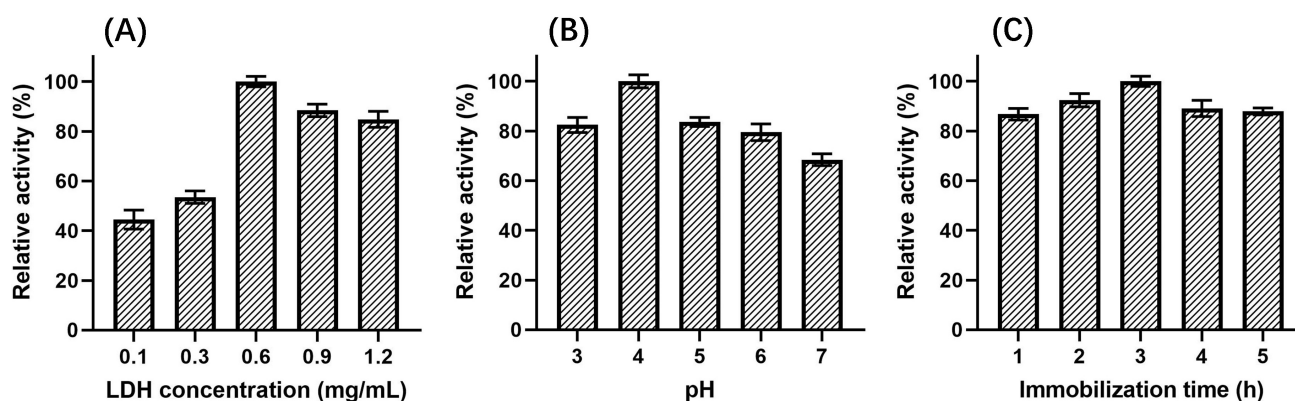


Fig. 5. Effect on relative activity of immobilized LDH. (A) LDH concentration. (B) pH. (C) Immobilization time.

was investigated, as shown in Fig. 5A. The relative activity increased dramatically and reached a maximum as the enzyme concentration increased from 0.1–0.6 mg/mL. When the concentration continued to rise to 1.2 mg/mL, the relative activity decreased slowly. It showed that the activity of immobilized LDH increased with the increase in the number of LDH immobilized on the surface of Fe_3O_4 . However, the active site was hidden because of excess LDH.

The effect of immobilization pH, ranging from 3 to 7 (LDH concentration of 0.6 mg/mL, immobilization time 2 h), on the relative activity of immobilized LDH was also investigated. As shown in Fig. 5B, when the pH changed from 3 to 4, the relative activity of immobilized LDH increased and reached a maximum. However, when the pH increased to 7, the activity of immobilized LDH gradually decreased, which might be caused by the increase of the electrostatic repulsion between LDH and the magnetic nanomaterials.

Different immobilization times were also investigated, ranging from 1 h to 5 h (LDH concentration of 0.6 mg/mL, pH 5), as shown in Fig. 5C. The relative activity increased gradually with time from 1–3 h. When the immobilization time was 3 h, the relative activity reached the maximum, but when the immobilization time was extended from 3 to 5 h, the relative activity decreased slightly. Thus, this illustrated that extension of time beyond 3 h was not conducive to the immobilization of LDH.

Compared with the enzyme immobilization conditions in other studies, our conditions were optimized, especially the immobilization time was greatly shortened to 3 h. For example, when immobilized beta-secretase was used to screen for potential inhibitors in *Dendrobii Caulis*, the enzyme required 24 h to immobilize on magnetic beads [35]. Immobilization of neuraminidase on the surface of magnetic beads required an overnight incubation in 500 μL of coupling buffer [36]. Furthermore, the N-terminus of angiotensin-converting enzyme required 16 h to covalently bind to the surface of glutaraldehyde-modified ferrite beads [37].

3.2.2 Response Surface Methodology (RSM) to Optimize the Operative Parameters

On the basis of the results of the single factor experiments, a response surface test was performed, and Design Expert software (version 8.0, Stat-Ease Inc., Minneapolis, MN, USA) was used to analyze the results. The relative activity of LDH reached the maximum when the pH was 4.43, the LDH concentration was 0.75 mg/mL, and the immobilization time was 3.49 h (Fig. 6). Simultaneously, the analysis of variance showed that $F = 7.27$, $p < 0.008$, and $R^2 > 0.90$, indicated that the response model was highly significant and fit well with the actual test. The coefficient of variation was $< 5.03\%$, proving that the model had good repeatability. The above results showed that the established model could reflect the relationship between variables and response values. As could be seen from Eqn. 3, LDH concentration had the greatest effect on relative activity, followed by time and pH. In summary, we further adjusted the conditions to LDH concentration of 0.7 mg/mL, pH of 4.5 and immobilization time of 3.5 h, and used it in subsequent experiments.

$$Y = 94.01 + 4.34 A + 3.06 B + 3.60 C + 2.74 AB + 6.23 AC - 0.57 BC - 8.75 A^2 - 4.75 B^2 - 6.60 C^2 \quad (3)$$

(Where Y represents the relative activity, A, B, C are the LDH concentration, pH and time, respectively.)

3.3 The Relationship between LDH Immobilization Yield and Other Parameters

First, the Coomassie brilliant blue method was used to determine the standard curve of LDH content, which was $Y = 0.0438X + 0.0129$ ($R^2 = 0.995$); it was used for the calculation of the subsequent LDH immobilization yield.

Three factors, including LDH concentration, pH, and immobilization time, were investigated to explore the relationship with the LDH immobilization yield. As could be seen in Fig. 7, the yield increased first and then decreased with the increase in LDH concentration, and when the con-

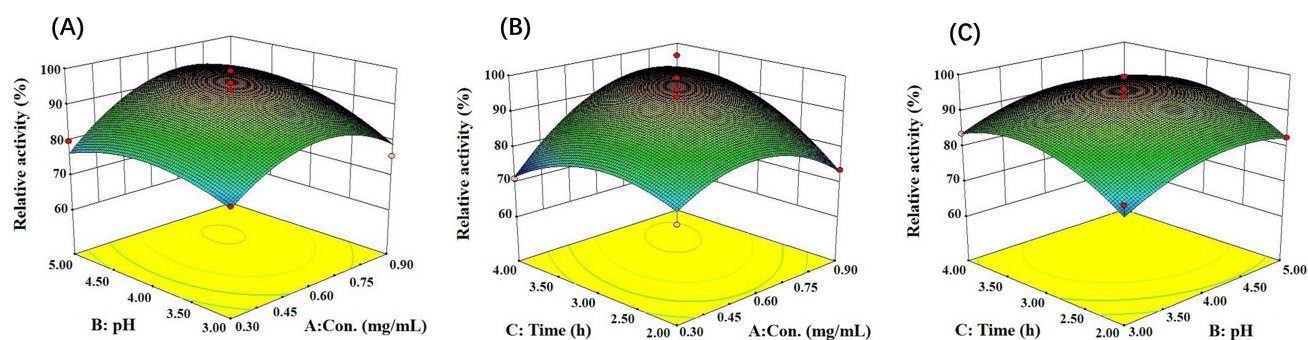


Fig. 6. Response surfaces and contour plots show the interaction of reaction conditions on immobilized LDH activity. (A) Concentration and pH. (B) Concentration and time. (C) Time and pH.

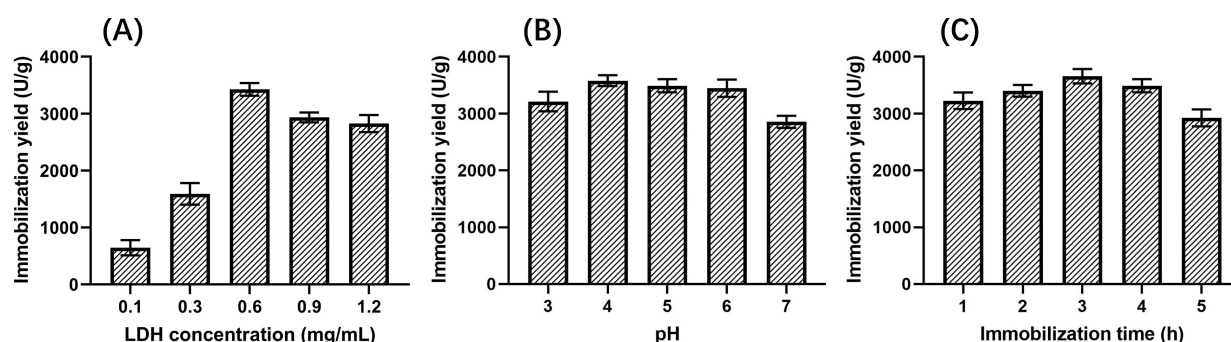


Fig. 7. Effects on the yield of immobilized LDH. (A) LDH concentration. (B) pH. (C) Immobilization time.

centration was 0.6 mg/mL, the yield reached a maximum value of $(3.43 \pm 0.11) \times 10^3$ U/g. At the same time, the immobilization yield of LDH remained unchanged in the pH range of 3–6 and reached a maximum of $(3.58 \pm 0.10) \times 10^3$ U/g at pH 4; however, as the pH increased to 7, the immobilization yield significantly dropped to $(2.86 \pm 0.07) \times 10^3$ U/g (Fig. 7B). The immobilization yield reached a maximum value of $(3.66 \pm 0.13) \times 10^3$ U/g when the immobilization time was 3 h (Fig. 7C).

The optimal conditions for activity of immobilized LDH were determined in single-factor experiments and the response surface test described in Section 3.2. These conditions that were used for screening were an LDH concentration of 0.7 mg/mL, a pH value of 4.5, and an immobilization time of 3.5 h. Under these conditions, the immobilized yield of LDH was $(3.79 \pm 0.08) \times 10^3$ U/g.

The peroxxygenase was immobilized on monoaminoethyl-N-aminoethyl activated agarose beads, and the immobilized yield of the enzyme was 7.5×10^2 U/g after optimizing the conditions [38]. The rhamnosidase was immobilized on the magnetic metal-organic framework using a cross-linker, and the immobilization yield of the enzyme was 8.17×10^2 U/g [39]. Compared with the above experiments, the immobilization yield of LDH was ~5 times greater.

3.4 Operative Parameters Optimization for Immobilized LDH Ligand Screening

Since chlorogenic acid could not bind to LDH, it was selected as a negative control, while galloflavin was selected as a positive control [40]. Therefore, a model mixture (containing galloflavin and chlorogenic acid) was used to test the specificity of immobilized LDH. This mixture model was then also used to optimize the experimental conditions for ligand fishing of immobilized LDH.

The specificity experimental results of immobilized LDH are shown in Fig. 8A. S2–S4 were the washing solutions of the buffer solution, and no substance was detected in S4, indicating that the components not bound to the immobilized LDH could be completely washed away after washing three times. S5–S7 were methanol eluates, in which only the positive control drug galloflavin was detected, while the negative control drug chlorogenic acid was not detected, proving that the immobilized LDH ligand was specific for ligand fishing.

Then, the optimal incubation time between 10–60 min was selected as shown in Fig. 8B. When the incubation time was extended from 10 min to 30 min, the peak area of galloflavin increased significantly and reached the maximum. The peak area decreased slightly at the 40 min incubation time. However, as the incubation time was further increased to 60 min, the peak area decreased substantially. This result indicated that the active site of LDH reached saturation after 30 min of incubation.

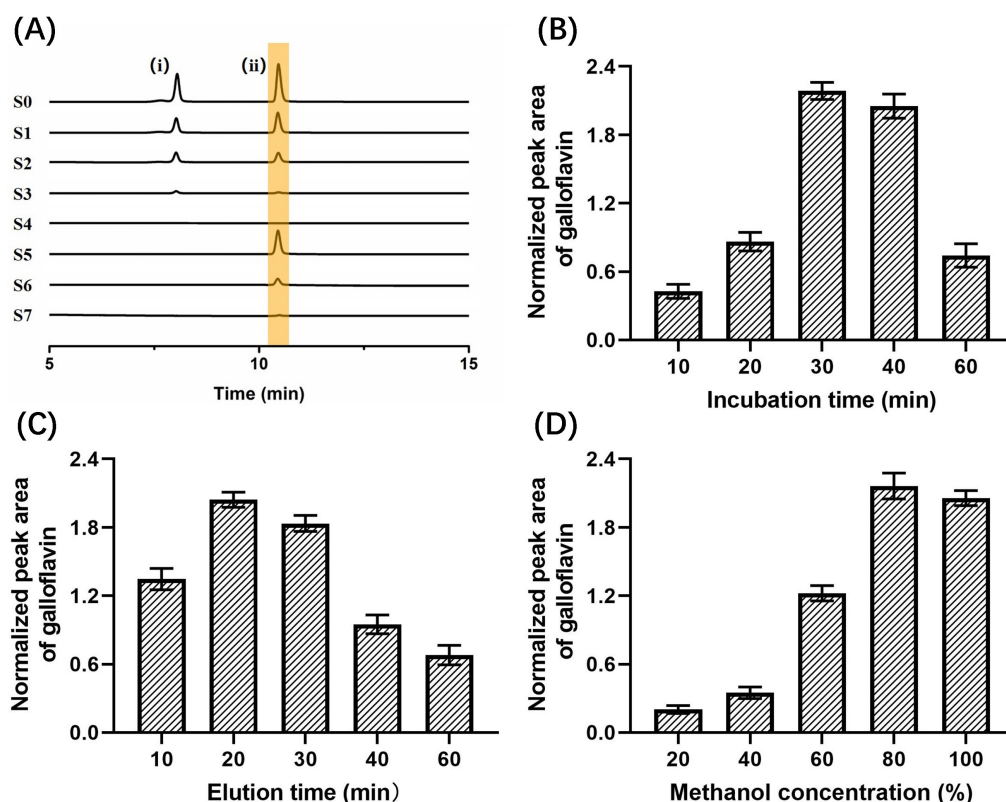


Fig. 8. Effects on the binding efficiency of galloflavin. (A) Base peak chromatograms acquired from different solutions (S0–S7) during the developed LDH-MNPs-based ligand fishing procedure from a model mixture containing chlorogenic acid (i), galloflavin (ii). (B) Incubation times. (C) Elution time. (D) Methanol concentration.

As shown in Fig. 8C, the optimal resolution time between 10–60 min was 20 min. The peak area of galloflavin showed a trend of increasing first and then decreasing. When the elution time exceeded 20 min, the peak area gradually decreased. This phenomenon that was observed over time could have occurred because galloflavin was encapsulated by agglomerated and precipitated enzyme molecules for too long, resulting in a decrease in the peak area.

The optimal methanol concentration was obtained by investigating different methanol concentrations (20%, 40%, 60%, 80%, and 100%). When the methanol concentration increased from 20%–80%, the peak area gradually increased and reached the maximum value. However, the peak area decreased at 100% (Fig. 8D). It proved that 80% methanol was favorable for the elution of galloflavin.

In addition, the specificity of immobilized enzymes has also been investigated in other published studies. For example, cyclooxygenase-2 (COX-2) immobilized on nickel ion (Ni_2^{+}) functionalized magnetic mesoporous silica microspheres could specifically bind to celecoxib in a mixed system of celecoxib (a COX-2 inhibitor) and phlozizin (a noninhibitor) [41]. The reactor made by immobilizing AChE on the capillary could specifically screen out galantamine (AChE inhibitor) in the mixed system of an AChE inhibitor and a non-inhibitor [42]. Porcine pancreatic lipase was immobilized on a metal-organic frame-

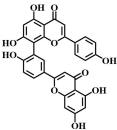
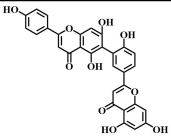
work UiO-66- NH_2 using precipitant cross-linking, and hesperidin was specifically bound using a mixed system of hesperidin and gallic acid (a lipase inhibitor and non-inhibitor, respectively) [43].

3.5 Ligand Fishing Assay for *Selaginella doederleinii* Ethyl Acetate Extract

The utility of immobilized LDH was further confirmed by screening potential inhibitors of LDH in *Selaginella doederleinii* ethyl acetate extracts using the ligand fishing method. The experimental results are shown in Fig. 9. Under optimal conditions, two compounds were screened in the final elution step. Subsequently, these two compounds were confirmed as amentoflavone and robustaflavone using the UPLC/quadrupole time-of-flight (Q-TOF)-MS identification method and comparison with MS data and related standards (As shown in Table 2).

Amentoflavone could effectively inhibit the content of LDH, exert antioxidant effects and reduce hepatotoxicity. According to Li's report [44], 5 biflavonoids were isolated from *Hedyotis diffusa*. Among them, amentoflavone could significantly reduce the LDH content by the experiment of hydrogen peroxide-induced hepatocyte injury. Especially, the LDH content decreased from 580 U/L to 286 U/L when amentoflavone was 250 $\mu\text{mol/L}$. At the same time, the content of reactive oxygen species (ROS) was also reduced,

Table 2. The retention times and MS characteristics of the affinity ligands of *Selaginella doederleinii* acetate extract incubated with immobilized LDH.

No.	t_R /min	Analyte	Chemical structure	Neutral	Determined	Product ions (m/z)	Delta (ppm)	Formula
				Mass (Da)	$[M-H]^-$ (m/z)			
1	4.27	Amentoflavone		538.0658	537.0639	419.1025, 401.0351, 375.0682, 153.1011, 121.1264	-3.7	$C_{30}H_{18}O_{10}$
2	5.09	Robustaflavone		538.0846	537.0837	411.0897, 385.0461, 268.1167	-2.0	$C_{30}H_{18}O_{10}$

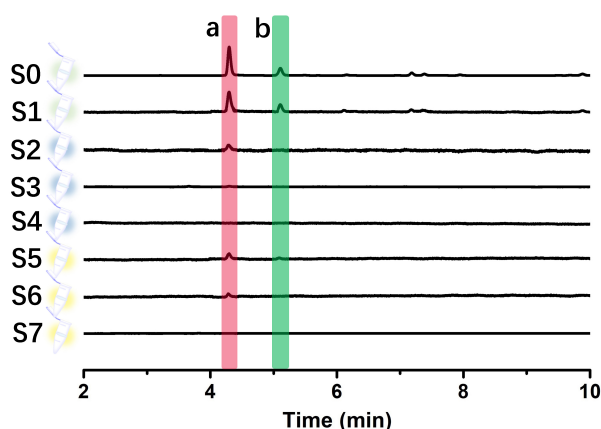


Fig. 9. UPLC chromatograms of different solutions (S0–S7) were obtained from the ethyl acetate extract of *Selaginella doederleinii* by an immobilized LDH-based ligand fishing approach.

which reduced liver cells damage and kept cells in a stable redox balance state. Oxidative damage is one of the mechanisms of tumorigenesis. Under normal conditions, ROS in the human body participates in normal physiological metabolism. There is a system that inhibited free radical reaction in the body, so that excessive free radicals in the body are scavenged [45]. However, if this reaction system is damaged, excessive free radicals will directly cause damage to human cells [46]. It could be seen that the generation of oxidative stress in organisms is caused by the increase in the number of free radicals or the decline in the antioxidant defense function [47].

Up to now, many literatures have reported that amentoflavone not only has anti-tumor effects, but also has low toxicity to human normal cells. For example, amentoflavone had a certain inhibitory effect on the proliferation of human malignant melanoma A-375 cells with an IC_{50} value of 240 $\mu\text{mol/L}$ [48]. When ovarian cancer cells SKOV3 and OVCAR-3 were treated with 50 $\mu\text{mol/L}$ amentoflavone for 72 h, the viability decreased by 31% and 35%, respectively [49]. The IC_{50} values of amentoflavone on human breast cancer MCF-7 BUS and MDA-MB-231

cells were 30.4 $\mu\text{mol/L}$ and 70 $\mu\text{mol/L}$, respectively, while the IC_{50} value of normal breast epithelial MCF-10A cells was 99 $\mu\text{mol/L}$ [50]. Amentoflavone at a concentration of 11.5–184.3 $\mu\text{mol/L}$ was used to treat human breast cancer MCF-7 cells and human peripheral lymphocytes (HPL). The inhibition rate of MCF-7 cells was dose-related with the concentration of amentoflavone, and its survival rate was reduced to 26.55% at a concentration of 184.3 $\mu\text{mol/L}$. At this concentration, the survival rate of HPL was 76%, indicating that amentoflavone was not toxic to normal cell lines and could be used as an anticancer drug [51]. Based on the above results, it can be speculated that further studies on amentoflavone as a potential anticancer drug are needed.

Compared with traditional screening methods, including chemical composition isolation and activity tracking [52], serum pharmacochimistry and network pharmacology [53], spectrum-effect relationship analysis and molecular docking [54], ligand fishing technology [55] could directly and accurately fishing out the active ingredients from complex natural products, simplifying the experimental steps and consuming less sample volume, further highlighting the specificity and efficiency of the technology.

4. Conclusions

Natural medicines have become the main source of modern new drug research and development because of their rich resources, diverse components, and wide range of biological activities. However, the traditional screening process is time-consuming and inefficient, which hinders the development of traditional Chinese medicines. Now, the ligand fishing technology with the advantages of fast screening speed, simple operation, and good specificity makes it suitable for screening potential active ingredients from multi-component systems, which has attracted more and more researchers' attention.

Therefore, we have shown that by immobilizing LDH on the surface of amino-modified magnetic nanomaterials, potential LDH inhibitors from traditional Chinese medicines could be targeted and screened. First, we opti-

mized the immobilization conditions for LDH using single-factor experiments and response surface methodology to obtain the maximum enzymatic activity and calculated the immobilization yield. Next, we used known LDH ligands and non-ligands to detect the specificity of immobilized LDH to further optimize the ligand fishing conditions. Finally, the immobilized LDH was applied for the first time to the screening of LDH ligands in ethyl acetate extracts of *Selaginella doederleinii* and combined with UPLC/Q-TOF-MS; we successfully identified two potential LDH inhibitors. These results show that ligand fishing is an effective method to screen natural products.

Author Contributions

GW, SL, FZ and HL designed the research study. FZ and HL performed the research. CL, KF and YJ provided help and advice on research protocols, data interpretation and discussion. MW, SX, LZ and JY analyzed the data. FZ wrote the manuscript. All authors contributed to editorial changes in the manuscript. All authors read and approved the final manuscript.

Ethics Approval and Consent to Participate

Not applicable.

Acknowledgment

Not applicable.

Funding

This research was funded by the 2018 National Science Foundation of China 81860697, Zunyi Talent Team Project (2020) No.10(E-361), Guizhou Province Science and Technology Plan Project [2020]4Y086.

Conflict of Interest

The authors declare no conflict of interest.

References

- [1] Sung H, Ferlay J, Siegel RL, Laversanne M, Soerjomataram I, Jemal A, *et al.* Global cancer statistics 2020: GLOBOCAN estimates of incidence and mortality worldwide for 36 cancers in 185 countries. *CA: A Cancer Journal for Clinicians*. 2021; 71: 209–249.
- [2] Al-Rashidi HE, Refaat S, Ahmed E, Hussein DT, Eltantawy FM, Hamed S. Involvement of INF- γ functional single nucleotide polymorphism +874 T/a (rs2430561) in breast cancer risk. *Saudi Journal of Biological Sciences*. 2021; 28: 6289–6296.
- [3] Huang X, Mahmudul HM, Li Z, Deng X, Su X, Xiao Z, *et al.* Noble metal nanomaterials for the diagnosis and treatment of hematological malignancies. *Frontiers in Bioscience-Landmark*. 2022; 27: 040.
- [4] Naviglio S. Lactic dehydrogenase and cancer an overview. *Frontiers in Bioscience*. 2015; 20: 1234–1249.
- [5] Jurisic V, Radenkovic S, Konjevic G. The Actual Role of LDH as Tumor Marker, Biochemical and Clinical Aspects. *Advances in Cancer Biomarkers*. 2015; 867: 115–124.
- [6] Koiri RK. Lactate as a signaling molecule Journey from dead end product of glycolysis to tumor survival. *Frontiers in Bioscience-Landmark*. 2019; 24: 366–381.
- [7] Varma G, Seth P, Souza PC, Callahan C, Pinto J, Vaidya M, *et al.* Visualizing the effects of lactate dehydrogenase (LDH) inhibition and LDH-A genetic ablation in breast and lung cancer with hyperpolarized pyruvate NMR. *NMR in Biomedicine*. 2021; 34: e4560.
- [8] Zhang Y, Li J, Wang B, Chen T, Chen Y, Ma W. LDH-a negatively regulates dMMR in colorectal cancer. *Cancer Science*. 2021; 112: 3050–3063.
- [9] Mishra D, Banerjee D. Lactate Dehydrogenases as Metabolic Links between Tumor and Stroma in the Tumor Microenvironment. *Cancers*. 2019; 11: 750.
- [10] Xian Z, Liu J, Chen Q, Chen H, Ye C, Xue J, *et al.* Inhibition of LDHA suppresses tumor progression in prostate cancer. *Tumor Biology*. 2015; 36: 8093–8100.
- [11] Han RL, Wang FP, Zhang PA, Zhou XY, Li Y. MiR-383 inhibits ovarian cancer cell proliferation, invasion and aerobic glycolysis by targeting LDHA. *Neoplasma*. 2017; 64: 244–252.
- [12] Fang ZX, He LQ, Jia H, Huang QS, Chen D, Zhang ZW. The miR-383-LDHA axis regulates cell proliferation, invasion and glycolysis in hepatocellular cancer. *Iranian Journal of Basic Medical Sciences*. 2017; 20: 187–192.
- [13] Cui XG, Han ZT, He SH, Wu XD, Chen TR, Shao CH, *et al.* HIF1/2 α mediates hypoxia-induced LDHA expression in human pancreatic cancer cells. *Oncotarget*. 2017; 8: 24840–24852.
- [14] Huang Y, Zhao J, Song Q, Zheng L, Fan C, Liu T, *et al.* Virtual screening and experimental validation of novel histone deacetylase inhibitors. *BMC Pharmacology and Toxicology*. 2016; 17: 32.
- [15] Wang L, Jiang Z, Xiao P, Sun J, Bi Z, Liu E. Identification of anti-inflammatory components in *Sinomenii Caulis* based on spectrum-effect relationship and chemometric methods. *Journal of Pharmaceutical and Biomedical Analysis*. 2019; 167: 38–48.
- [16] Yuan Y, Bai X, Liu Y, Tang X, Yuan H, Liao X. Ligand fishing based on cell surface display of enzymes for inhibitor screening. *Analytica Chimica Acta*. 2021; 1156: 338359.
- [17] Zhuo RJ, Liu H, Liu NN, Wang Y. Ligand Fishing: A Remarkable Strategy for Discovering Bioactive Compounds from Complex Mixture of Natural Products. *Molecules*. 2016; 21: 1516.
- [18] Guo H, Chen Y, Song N, Yang X, Yao S, Qian J. Screening of lipase inhibitors from bamboo leaves based on the magnetic ligand fishing combined with HPLC/MS. *Microchemical Journal*. 2020; 153: 104497.
- [19] Petersen MJ, Lima RDL, Kjaerulff L, Staerk D. Immobilized alpha-amylase magnetic beads for ligand fishing: Proof of concept and identification of alpha-amylase inhibitors in *Ginkgo biloba*. *Phytochemistry*. 2019; 164: 94–101.
- [20] Zhang F, Li SH, Liu C, Fang K, Jiang YM, Zhang JY, *et al.* Rapid screening for acetylcholinesterase inhibitors in *Selaginella doederleinii* Hieron by using functionalized magnetic Fe₃O₄ nanoparticles. *Talanta*. 2022; 243: 123284.
- [21] Lee N, Min H, Lee J, Nam J, Lee Y, Han A, *et al.* Identification of a New Cytotoxic Biflavone from *Selaginella doederleinii*. *Chemical and Pharmaceutical Bulletin*. 2008; 56: 1360–1361.
- [22] Reginaldo FPS, Costa ICD, Giordani RB. *Selaginellaceae*: traditional use, phytochemistry and pharmacology. *Boletim Latinoamericano Y Del Caribe De Plantas Medicinales Y Aromaticas*. 2020; 19: 247–288.
- [23] Li SG, Wang XW, Wang G, Shi PY, Lin SL, Xu DF, *et al.* Ethyl Acetate Extract of *Selaginella doederleinii* Hieron Induces Cell Autophagic Death and Apoptosis in Colorectal Cancer via PI3K-Akt-mTOR and AMPK α -Signaling Pathways. *Frontiers in Pharmacology*. 2020; 11: 565090.
- [24] Sui Y, Li S, Shi P, Wu Y, Li Y, Chen W, *et al.* Ethyl acetate extract from *Selaginella doederleinii* Hieron inhibits the growth of

- human lung cancer cells a549 via caspase-dependent apoptosis pathway. *Journal of Ethnopharmacology*. 2016; 190: 261–271.
- [25] Thomford NE, Senthebane DA, Rowe A, Munro D, Seele P, Maroyi A, *et al.* Natural Products for Drug Discovery in the 21st Century: Innovations for Novel Drug Discovery. *International Journal of Molecular Sciences*. 2018; 19: 1578.
 - [26] Wang G, Li SH, Zhou HL, Jiang YM, Shen MM, Yang LJ, *et al.* Phytochemical screening, antioxidant, antibacterial and cytotoxic activities of different extracts of *Selaginella doederleinii*. *Bangladesh Journal of Botany*. 2017; 46: 1193–1201.
 - [27] Feng J, Yu S, Li J, Mo T, Li P. Enhancement of the catalytic activity and stability of immobilized aminoacylase using modified magnetic Fe₃O₄ nanoparticles. *Chemical Engineering Journal*. 2016; 286: 216–222.
 - [28] Cheng G, Pi Z, Zheng Z, Liu S, Liu Z, Song F. Magnetic nanoparticles-based lactate dehydrogenase microreactor as a drug discovery tool for rapid screening inhibitors from natural products. *Talanta*. 2020; 209: 120554.
 - [29] Liu D, Xu B, Dong C. Recent advances in colorimetric strategies for acetylcholinesterase assay and their applications. *TrAC Trends in Analytical Chemistry*. 2021; 142: 116320.
 - [30] Idris AM, El-Zahhar AA. Indicative properties measurements by SEM, SEM-EDX and XRD for initial homogeneity tests of new certified reference materials. *Microchemical Journal*. 2019; 146: 429–433.
 - [31] Trayner S, Hao A, Downes R, Park JG, Su Y, Liang R. High-resolution TEM analysis of flattened carbon nanotube packing in nanocomposites. *Synthetic Metals*. 2015; 204: 103–109.
 - [32] Pakharukova VP, Yatsenko DA, Shalygin AS, Gerasimov EY, Tsybulya SV, Martyanov ON. XRD characterization of structural evolution and morphology properties of silica-doped alumina aerogels. *Acta Crystallographica Section A Foundations and Advances*. 2015; 71: s380–s381.
 - [33] Liu D, Chen J, Shi Y. Tyrosinase immobilization on aminated magnetic nanoparticles by physical adsorption combined with covalent crosslinking with improved catalytic activity, reusability and storage stability. *Analytica Chimica Acta*. 2018; 1006: 90–98.
 - [34] Meng Y, Yao C, Xue S, Yang H. Application of Fourier transform infrared (FT-IR) spectroscopy in determination of microalgal compositions. *Bioresource Technology*. 2014; 151: 347–354.
 - [35] Ye L, Zhang R, Cao J. Screening of β -secretase inhibitors from *Dendrobii Caulis* by covalently enzyme-immobilized magnetic beads coupled with ultra-high-performance liquid chromatography. *Journal of Pharmaceutical and Biomedical Analysis*. 2021; 195: 113845.
 - [36] Zhao Y, Wang L, Luo S, Wang Q, Moaddel R, Zhang T, *et al.* Magnetic beads-based neuraminidase enzyme microreactor as a drug discovery tool for screening inhibitors from compound libraries and fishing ligands from natural products. *Journal of Chromatography a*. 2018; 1568: 123–130.
 - [37] de Almeida FG, Vanzolini KL, Cass QB. Angiotensin converting enzyme immobilized on magnetic beads as a tool for ligand fishing. *Journal of Pharmaceutical and Biomedical Analysis*. 2017; 132: 159–164.
 - [38] Carballares D, Morellon-Sterling R, Xu X, Hollmann F, Fernandez-Lafuente R. Immobilization of the Peroxygenase from *Agroclybe aegerita*. The Effect of the Immobilization pH on the Features of an Ionically Exchanged Dimeric Peroxygenase. *Catalysts*. 2021; 11: 560.
 - [39] Zhu MS, Wang SM, inventor. A method for preparing hesperetin dihydrochalcone glucoside by immobilized enzyme method. CHN: China patent CN20211122757. 4 January 2022.
 - [40] Han X, Sheng X, Jones HM, Jackson AL, Kilgore J, Stine JE, *et al.* Evaluation of the anti-tumor effects of lactate dehydrogenase inhibitor galloflavin in endometrial cancer cells. *Journal of Hematology & Oncology*. 2015; 8: 2.
 - [41] Li D, Xu L, Qi J, Yu B. Screening and analysis of cyclooxygenase-2 inhibitors from the complex matrix: a case study to illustrate the important effect of immobilized enzyme activity in magnetic ligand fishing. *Journal of Pharmaceutical and Biomedical Analysis*. 2019; 175: 112795.
 - [42] Wang L, Zhao Y, Zhang Y, Zhang T, Kool J, Somsen GW, *et al.* Online screening of acetylcholinesterase inhibitors in natural products using monolith-based immobilized capillary enzyme reactors combined with liquid chromatography-mass spectrometry. *Journal of Chromatography A*. 2018; 1563: 135–143.
 - [43] Chen X, Xue S, Lin Y, Luo J, Kong L. Immobilization of porcine pancreatic lipase onto a metal-organic framework, PPL@MOF: a new platform for efficient ligand discovery from natural herbs. *Analytica Chimica Acta*. 2020; 1099: 94–102.
 - [44] Li YL, Chen X, Niu SQ, Zhou HY, Li QS. Protective Antioxidant Effects of Amentoflavone and Total Flavonoids from *Hedyotis diffusa* on H₂O₂-Induced HL-O2 Cells through ASK1/p38 MAPK Pathway. *Chemistry & Biodiversity*. 2020; 17: e2000251.
 - [45] Vodicka P, Urbanova M, Makovicky P, Tomasova K, Kroupa M, Stetina R, *et al.* Oxidative Damage in Sporadic Colorectal Cancer: Molecular Mapping of Base Excision Repair Glycosylases in Colorectal Cancer Patients. *International Journal of Molecular Sciences*. 2020; 21: 2473.
 - [46] Taucher E, Mykoliuk I, Fediuk M, Smolle-Juettner FM. Autophagy, Oxidative Stress and Cancer Development. *Cancers*. 2022; 14: 1637.
 - [47] Klaunig JE. Oxidative Stress and Cancer. *Current Pharmaceutical Design*. 2018; 24: 4771–4778.
 - [48] Duan SL, Jia JF, Hong B, Zhou J, Zhang Y, Ge FH, *et al.* Assessment of Amentoflavone Loaded Sub-Micron Particle Preparation using Supercritical Antisolvent for its Antitumor Activity. *Current Drug Delivery*. 2022; 19: 41–48.
 - [49] Liu H, Yue Q, He S. Amentoflavone suppresses tumor growth in ovarian cancer by modulating Skp2. *Life Sciences*. 2017; 189: 96–105.
 - [50] Aliyev AT, Ozcan-Sezer S, Akdemir A, Gurer-Orhan H. In vitro evaluation of estrogenic, antiestrogenic and antitumor effects of amentoflavone. *Human & Experimental Toxicology*. 2021; 40: 1510–1518.
 - [51] L. S S, Nair BR. A simple protocol for the isolation of amentoflavone from two species of Biophytum DC. (Oxalidaceae) and evaluation of its antiproliferative potential. *Industrial Crops and Products*. 2021; 160: 113099.
 - [52] Lei J, Wang Y, Li W, Fu S, Zhou J, Lu D, *et al.* Natural green deep eutectic solvents-based eco-friendly and efficient extraction of flavonoids from *Selaginella moellendorffii*: Process optimization, composition identification and biological activity. *Separation and Purification Technology*. 2022; 283: 120203.
 - [53] Wei JX, Yu YY, Zhang Y, Li LZ, Li X, Shao J, *et al.* Integrated Serum Pharmacochimistry and Network Pharmacology Approach to Explore the Effective Components and Potential Mechanisms of Menisperm Rhizoma Against Myocardial Ischemia. *Frontiers in Chemistry*. 2022; 10: 869972.
 - [54] Zheng G, Gan L, Jia L, Zhou D, Bi S, Meng Z, *et al.* Screen of anti-migraine active compounds from *Duijinsan* by spectrum-effect relationship analysis and molecular docking. *Journal of Ethnopharmacology*. 2021; 279: 114352.
 - [55] Guo S, Wang S, Meng J, Gu DY, Yang Y. Immobilized enzyme for screening and identification of anti-diabetic components from natural products by ligand fishing. *Critical Reviews in Biotechnology*. 2022. (in press)